

University of Windsor

## Scholarship at UWindsor

---

Chemistry and Biochemistry Publications

Department of Chemistry and Biochemistry

---

9-10-2019

# Peptide-Induced Lipid Flip-Flop in Asymmetric Liposomes Measured by Small Angle Neutron Scattering

Michael H.L. Nguyen  
*University of Windsor*

Mitchell DiPasquale  
*University of Windsor*

Brett W. Rickeard  
*University of Windsor*

Milka Doktorova  
*University of Texas Health Science Center at Houston*

Frederick A. Heberle  
*University of Texas Health Science Center at Houston*

*See next page for additional authors*

Follow this and additional works at: <https://scholar.uwindsor.ca/chemistrybiochemistrypub>



Part of the [Biochemistry, Biophysics, and Structural Biology Commons](#), and the [Chemistry Commons](#)

---

### Recommended Citation

Nguyen, Michael H.L.; DiPasquale, Mitchell; Rickeard, Brett W.; Doktorova, Milka; Heberle, Frederick A.; Scott, Haden L.; Barrera, Francisco N.; Taylor, Graham; Collier, Charles P.; Stanley, Christopher B.; Katsaras, John; and Marquardt, Drew. (2019). Peptide-Induced Lipid Flip-Flop in Asymmetric Liposomes Measured by Small Angle Neutron Scattering. *Langmuir*, 35 (36), 11735-11744.  
<https://scholar.uwindsor.ca/chemistrybiochemistrypub/154>

This Article is brought to you for free and open access by the Department of Chemistry and Biochemistry at Scholarship at UWindsor. It has been accepted for inclusion in Chemistry and Biochemistry Publications by an authorized administrator of Scholarship at UWindsor. For more information, please contact [scholarship@uwindsor.ca](mailto:scholarship@uwindsor.ca).

---

## Authors

Michael H.L. Nguyen, Mitchell DiPasquale, Brett W. Rickeard, Milka Doktorova, Frederick A. Heberle, Haden L. Scott, Francisco N. Barrera, Graham Taylor, Charles P. Collier, Christopher B. Stanley, John Katsaras, and Drew Marquardt

# Peptide-Induced Lipid Flip-Flop in Asymmetric Liposomes Measured by Small Angle Neutron Scattering

Michael H.L. Nguyen,<sup>†</sup> Mitchell DiPasquale,<sup>†</sup> Brett W. Rickeard,<sup>†</sup> Milka  
Doktorova,<sup>‡</sup> Frederick A. Heberle,<sup>‡,¶</sup> Haden L. Scott,<sup>¶,§</sup> Francisco N. Barrera,<sup>§</sup>  
Graham Taylor,<sup>||</sup> Charles P. Collier,<sup>||,⊥</sup> Christopher B. Stanley,<sup>#</sup> John  
Katsaras,<sup>@,△,∇</sup> and Drew Marquardt<sup>\*,†,††</sup>

<sup>†</sup>*Department of Chemistry and Biochemistry, University of Windsor, Windsor, ON, Canada*

<sup>‡</sup>*Department of Integrative Biology and Pharmacology, University of Texas Health Science Center at  
Houston, Houston, TX, USA*

<sup>¶</sup>*Center for Environmental Biotechnology, University of Tennessee, Knoxville, TN, USA*

<sup>§</sup>*Department of Biochemistry & Cellular and Molecular Biology, University of Tennessee, Knoxville, TN,  
United States*

<sup>||</sup>*The Bredesen Center, University of Tennessee, Knoxville, TN, USA*

<sup>⊥</sup>*Center for Nanophase Materials Sciences, Oak Ridge National Laboratory, Oak Ridge, TN, USA*

<sup>#</sup>*Neutron Scattering Division, Oak Ridge National Laboratory, Oak Ridge, TN, USA*

<sup>@</sup>*Large Scale Structures Group, Oak Ridge National Laboratory, Oak Ridge, TN, USA*

<sup>△</sup>*Shull Wollan Center, a Joint Institute for Neutron Sciences, Oak Ridge National Laboratory, Oak Ridge,  
TN, USA*

<sup>∇</sup>*Department of Physics and Astronomy, University of Tennessee, Knoxville, TN, USA*

<sup>††</sup>*Department of Physics, University of Windsor, Windsor, ON, Canada*

E-mail: [drew.marquardt@uwindsor.ca](mailto:drew.marquardt@uwindsor.ca)

## Abstract

Despite the prevalence of lipid transbilayer asymmetry in natural plasma membranes, most biomimetic model membranes studied are symmetric. Recent advances

have helped to overcome the difficulties in preparing asymmetric liposomes *in vitro*, allowing for the examination of a larger set of relevant biophysical questions. Here, we investigate the stability of asymmetric bilayers by measuring lipid flip-flop with time-resolved small-angle neutron scattering (SANS). Asymmetric large unilamellar vesicles with inner bilayer leaflets containing predominantly 1-palmitoyl-2-oleoyl-sn-glycero-3-phosphocholine (POPC) and outer leaflets composed mainly of 1,2-dimyristoyl-sn-glycero-3-phosphocholine (DMPC), displayed slow spontaneous flip-flop at 37 °C (half-time,  $t_{1/2} = 140$  h). However, inclusion of peptides, namely gramicidin, alamethicin, melittin, or pHLIP (i.e., pH-low insertion peptide) accelerated lipid flip-flop. For three of these peptides (i.e., pHLIP, alamethicin, and melittin), each of which was added externally to pre-formed asymmetric vesicles, we observed a completely scrambled bilayer in less than 2 hours. Gramicidin, on the other hand, was pre-incorporated during the formation of the asymmetric liposomes and showed a time resolvable 8-fold increase in the rate of lipid asymmetry loss. These results point to a membrane surface-related (e.g. adsorption/insertion) event as the primary driver of lipid scrambling in the asymmetric model membranes of this study. We discuss the implications of membrane peptide binding, conformation, and insertion on lipid asymmetry.

## Introduction

In nature, the lipid bilayer leaflets of cell plasma membranes possess chemically distinct lipids from one another, thus making the overall membranes asymmetric (an example of a model asymmetric bilayer is depicted in Fig. 1a). Glycerophospholipids, a major component of lipid bilayers, can differ from one another as follows: (i) degree of acyl chain unsaturation

---

Notice of Copyright This manuscript has been authored by UT-Battelle, LLC under Contract No. DE-AC05-00OR22725 with the U.S. Department of Energy. The United States Government retains and the publisher, by accepting the article for publication, acknowledges that the United States Government retains a non-exclusive, paid-up, irrevocable, world-wide license to publish or reproduce the published form of this manuscript, or allow others to do so, for United States Government purposes. The Department of Energy will provide public access to these results of federally sponsored research in accordance with the DOE Public Access Plan (<http://energy.gov/downloads/doe-public-access-plan>).

and length; (ii) headgroup chemistry; and (iii) type of bond (ester or ether) connecting the acyl chains to their glycerol backbone. With differing glycerophospholipid compositions, physical and chemical differences arise between the bilayer leaflets, which affect membrane fluidity and structure and have been shown to influence membrane function and membrane-associated protein activity.<sup>1,2</sup>

Maintaining membrane asymmetry is energetically expensive for cells and is accomplished by ATP-fueled proteins such as flippases and floppases.<sup>3</sup> Loss of asymmetry can lead to cell death or apoptosis. Specifically, the migration of phosphatidylserine (PS) lipids from the inner to the outer bilayer leaflet is a trigger for phagocytosis of dying cells.<sup>4,5</sup> Interestingly, greater protein reconstitution rates and activities are seen when studying asymmetric liposomes when compared to their symmetric counterparts.<sup>6,7</sup> Thus, in recent years there are an increasing number of studies examining the role of lipid asymmetry on different proteins and peptides.<sup>8-10</sup> On the other hand, studies examining how macromolecules affect membrane asymmetry are much less common.<sup>10</sup>

Beyond the relevant enzymes present in cells, we address the role that antimicrobial peptides (AMPs) have on lipid flip-flop. AMPs are a highly conserved group of amphipathic peptides and an integral part of the immune system of most, if not all, species of life. Their mode of action is primarily based on disrupting key plasma membrane properties and functions, such as electrochemical gradients, cell motility, and shape through lysis.<sup>11</sup> In order to do so, many will first bind and then insert themselves into the membrane, sometimes forming higher ordered structures (e.g. pores) to permeabilize the membrane. However, under certain conditions they have also been shown to accelerate lipid flip-flop,<sup>10,12-16</sup> which is thought to be pertinent to their cytotoxic effects.<sup>17</sup> To our knowledge, no existing study decouples the role of peptide binding to membranes and their transmembrane inserted state on lipid flip-flop dynamics. **This study will shed light on the mechanism through which AMPs disrupt membranes, highlighting the possibility of lipid reorganization as a relevant cause of cell death.**

Considerable research has been performed on passive, active, and nonenzyme-catalyzed lipid flip-flop in order to gain an understanding of the energy needed to generate, maintain, and disrupt lipid asymmetry. Many of these studies used spin- or fluorescent-labeled lipids because of their widespread availability.<sup>3,12,18–20</sup> However, bulky fluorescent probes can potentially perturb the membrane and alter its physical properties, affecting lipid flip-flop in the process.<sup>21,22</sup> Furthermore, these techniques measure the translocation of the reporter lipid, which is physically and chemically different from the host lipid of interest.<sup>22</sup> As a result, probe-free techniques such as sum-frequency vibrational spectroscopy (SFVS)<sup>22,23</sup> and neutron reflectometry<sup>24</sup> have gained some prominence as they allow measurements of lipid kinetics without the use of extrinsic probes. Collectively, these techniques are sensitive to chemical differences in leaflets by using isotopically labeled lipids that better resemble those found in nature.

Recently, we developed a novel probe-free assay using proton NMR to measure the relative flip-flop rates of phosphatidylcholine (PC) lipids in stress- and defect-free unilamellar vesicle systems.<sup>25</sup> The passive flip-flop rates were measured in large unilamellar vesicles (LUVs) with an asymmetric distribution of isotopically-labeled phospholipids. Using this system, flip-flop rates were found to be orders of magnitudes slower than those measured on substrate-supported planar bilayers. The difference between the two sample preparations was attributed to incomplete substrate coverage in the case of planar bilayers that led to the formation of pore defects.<sup>25</sup> Unlike passive lipid flip-flop, pores allow lipids to move from one leaflet to the other without desolvating their headgroups by simple diffusion. The NMR approach, however, is currently limited to choline-containing lipid systems. Moreover, in the case of proteolipidic systems, charged amino acid residues can potentially chelate with the NMR shift reagent ( $\text{Pr}^{3+}$ ), adversely affecting not only the NMR signal, but also protein conformation, binding, insertion, and function. Currently, we are not aware of a probe-free technique that measures lipid flip-flop rates in asymmetric vesicles in a non-headgroup specific fashion.

To address this, we explored the use of SANS, a technique that is differentially sensitive to hydrogen's isotopes, namely protium and deuterium ( $^1\text{H}$  and  $^2\text{H}$ , respectively), to measure lipid flip-flop in PC bilayers. Isotopic substitution of  $^1\text{H}$  for  $^2\text{H}$  imparts neutron contrast to the system that can then be used to study structural and dynamical membrane features. For example, SANS has been used to study the existence of lipid domains in living bacterial membrane<sup>26</sup> and the thickness of membranes reconstituted from natural lipid sources,<sup>26,27</sup> including symmetric<sup>28</sup> and asymmetric model membranes.<sup>29-31</sup> Although the use of SANS to measure lipid flip-flop rates is not a novel concept,<sup>32</sup> until now it has only been applied to symmetric model membranes.<sup>32-36</sup> This is partly due to the technical difficulties associated with preparing asymmetric vesicles of sufficient amounts and concentrations,<sup>37,38</sup> and the complicated experimental set-up and subsequent analysis of scattering profiles.

Here we describe a novel SANS approach to measure lipid flip-flop in asymmetric LUVs (aLUVs). As a proof of concept, we first characterized aLUVs composed of PC lipids to ensure that the neutron scattering signal was sufficiently different from that of symmetric (scrambled) control samples. We then introduced peptides with different modes of membrane interactions. For example, gramicidin (gA) forms ion channels when dimerized, and at elevated concentrations, alamethicin (Alm) and melittin (Mel) form barrel-stave and toroidal pores, respectively.<sup>39</sup> Although pHLIP is not an AMP, it was chosen to represent both an unstructured peripheral peptide and a transmembrane helix, depending on pH. For example, at neutral pH, pHLIP adsorbs to the membrane surface but inserts into the membrane at low pH.<sup>40</sup> Initially, peptide influence on lipid asymmetry was tracked through the time-dependent loss of the scattering signal, indicative of increased lipid flip-flop that, ultimately, results in a scrambled bilayer. Importantly, the lipid scrambling effect was most pronounced when the peptides were externally added to aLUVs, compared to when incorporated during aLUV preparation. Our results lend insights to the study of proteolipidic systems, especially with regard to peptide binding, conformation, and insertion on lipid bilayer asymmetry.

# Materials and Methods

## Materials.

1,2-Dimyristoyl-d54-sn-glycero-3-phosphocholine [14:0(d27)/14:0(d27) PC, dC-DMPC] and 1-palmitoyl-2-oleoyl-sn-glycero-3-phosphocholine-d13 (16:0/18:1 PC-d13, dH-POPC) were purchased from Avanti Polar Lipids, Inc. (Alabaster, AL) and used as received. Methyl- $\beta$ -cyclodextrin (M $\beta$ CD) was purchased from Acros Organics (Thermo Fisher Scientific, Waltham, MA). The centrifugal filter device, Amicon Ultra-15, was purchased from EMD Millipore (Billerica, MA). 99.9% D<sub>2</sub>O and deuterated methanol (d-methanol) were purchased from Cambridge Isotopes (Andover, MA). Praseodymium (III) nitrate hexahydrate (Pr<sup>3+</sup>) was purchased from Alfa Aesar (Ward Hill, MA) and prepared as a 20 mM stock solution in D<sub>2</sub>O. Alamethicin and melittin were purchased from Sigma-Aldrich (St. Louis, MO) and kept as stock solutions in d-methanol. Gramicidin was purchased as a lyophilized powder from Sigma-Aldrich (Oakville, ON, Canada) and kept as a stock solution in methanol. pHLIP was purchased as a lyophilized powder from P3 Biosystems (Louisville, KY) with 95% purity as verified by reverse-phase high performance liquid chromatography (HPLC). Sodium deuterioxide (NaOD) and deuterium chloride (DCl) were purchased from Sigma-Aldrich (St. Louis, MO).

## Preparation of Asymmetric LUV Samples

aLUVs were prepared using a slightly modified methyl- $\beta$ -cyclodextrin mediated exchange protocol to that outlined by Doktorova *et al.*<sup>29,37</sup> Briefly, dC-DMPC and dH-POPC in HPLC-grade chloroform were dried into separate lipid films under a stream of nitrogen gas, and left overnight *in vacuo* to remove any traces of solvent. The dC-DMPC and dH-POPC films were then hydrated using 20% (w/w) sucrose and 20 mM NaCl solutions, respectively. dH-POPC acceptor LUVs ( which “accepts” outer leaflet lipids from donor vesicles) were extruded (31 passes) using 100 nm pore diameter disposable polycarbonate membranes (NanoSizer

extruder, T&T Scientific). In the presence of M $\beta$ CD (at M $\beta$ CD:donor nominal ratio of 8:1), dC-DMPC donor multilamellar vesicles (MLVs) were incubated for one hour with acceptor dH-POPC LUVs (at a 3:1 donor-to-acceptor molar ratio) to promote outer leaflet exchange. During this process, aLUVs with dH-POPC primarily in the inner leaflet and dC-DMPC in the outer leaflet gradually form from the acceptor LUVs. Following this, aLUVs were purified through a combination of centrifugation and centrifugal filtration where the H<sub>2</sub>O buffer solution was exchanged for D<sub>2</sub>O to reduce neutron background signal. The final concentration of aLUVs was determined to be 17 mg/mL based on total intensity measured by dynamic light scattering (DLS) versus samples of known concentrations.

gA from a methanol stock solution was added at a peptide-to-lipid (P/L) molar ratio of 1/40 during the lipid film preparation step (i.e. pre-incorporated into the acceptor vesicles as described in Doktorova *et al.*<sup>10</sup>). It should be noted that the addition of gA in methanol to pre-formed aLUVs resulted in instantaneous peptide aggregation and was thus not used. In contrast, Alm and Mel precipitated out of solution during the centrifugation steps of the asymmetric vesicle preparation, and could not be incorporated directly into asymmetric bilayers, as was done in the case of gA. Alm and Mel were therefore introduced to pre-formed aLUVs using d-methanol at a P/L ratio of 1/40. The d-methanol concentration in the sample was  $\sim$ 3% (v/v), which, by itself, did not induce scrambling in aLUVs (see Fig. S4). As previously described, monomeric pHLIP transitions from a mostly unstructured peptide adsorbed to the membrane to an  $\alpha$ -helical conformation when it inserts into the membrane at low pH.<sup>41,42</sup> In order to take advantage of these pH-sensitive conformers, aLUVs in a 10 mM sodium phosphate buffer solution (pH 7.9) were added to a lyophilized pHLIP powder (weighed mass) at a P/L ratio of 1/150 and incubated for up to an hour. Afterwards, the pH of the different aLUVs preparations was adjusted to alter pHLIP's resulting orientation from one that is membrane adsorbed (pH 7.9) to a transmembrane orientation (pH 4.6). Measurements at pH 6.0 were also performed to capture any intermediate state(s) of pHLIP.<sup>40</sup> pHLIP's secondary structures in these different pH conditions was determined using circular

dichroism (Fig. S3).

## Quantifying aLUV Composition by GC/MS and solution $^1\text{H}$ NMR.

To determine the lipid exchange efficiency of the asymmetric sample preparation, aLUV lipid compositions were analyzed using a combination of gas chromatography/mass spectrometry (GC/MS) and  $^1\text{H}$  NMR. A small aliquot of  $\sim 20$   $\mu\text{g}$  lipids was subjected to transesterification using acid-catalyzed methanolysis.<sup>29</sup> The relative populations of the free fatty acid chains were determined using GC/MS<sup>29</sup> to yield the overall fraction of dC-DMPC and dH-POPC. GC/MS measurements were performed on an Agilent 5890A gas chromatograph (Santa Clara, CA) outfitted with a 5975C mass spectrometer. Taking advantage of the unique retention times of chemically distinct acyl chains, aLUVs were determined to possess 38% dC-DMPC and 62% dH-POPC. The exchange efficiency of the asymmetric prep was thus 76%, in good agreement with previous reports.<sup>25,29,43</sup>

$^1\text{H}$  NMR was used to determine the interleaflet lipid distribution of dC-DMPC and, combined with the GC/MS results, the overall lipid composition of each leaflet. NMR measurements were carried out at  $50^\circ\text{C}$  with an Avance III 600 MHz spectrometer (Bruker, Billerica, MA). Spectra were acquired using the Bruker TopSpin software and analyzed using TopSpin 3.5. The outer and inner leaflet distribution of protiated PC headgroups was determined through the addition of a 2  $\mu\text{L}$  aliquot of 20 mM  $\text{Pr}^{3+}$  into 700  $\mu\text{L}$  of aLUVs with a concentration of  $\sim 1$  mg/mL. The addition of  $\text{Pr}^{3+}$  causes outer leaflet choline peaks to shift downfield. NMR spectra were fit with a sum of Lorentzians; the peaks representing the inner and outer leaflet cholines were then integrated to determine their areas, which are directly proportional to the mol fraction of dC-DMPC in the outer and inner bilayer leaflets (0.87 and 0.13, respectively). NMR spectra are shown in Fig. S1. The fact that some donor dC-DMPC is present in the inner leaflet is not unexpected and in line with previous observations.<sup>37</sup> A summary of the NMR data can be found in Table S1 of the Supporting Information.

## aLUV Structure Determined by DLS and Small Angle Scattering

DLS measurements to determine vesicle integrity in the presence of peptides and solvent as a function of time were conducted on a Brookhaven BI-200SM system (Brookhaven Instruments, Holtsville, NY). For the DLS measurements, aLUVs at a concentration of 17 mg/mL were diluted by a factor of 1000 using ultrapure water and measured at room temperature. Small angle X-ray scattering (SAXS) experiments on aLUV and aLUV-peptide samples at 17 mg/mL were performed using a Rigaku BioSAXS-2000 (Rigaku Americas, The Woodlands, TX) equipped with a Pilatus 100K detector and an HF007 rotating copper anode. Several measurements of each sample were conducted at 37°C and examined for radiation damage before averaging. SAXS and SANS data (of the first time points) were jointly refined using an asymmetric six-slab model that accounts for contributions from the lipid headgroups, acyl chains, and terminal methyls of each leaflet to derive the structural parameters shown in Fig. S2.<sup>30</sup> aLUV control samples were well-fit by the asymmetric model, while those containing peptides were best-fit by a symmetric bilayer.

## Time-Resolved Flip-Flop using SANS

SANS measurements were conducted on the extended Q-range small angle neutron scattering (EQ-SANS) diffractometer located at the Spallation Neutron Source, Oak Ridge National Laboratory (ORNL, Oak Ridge, TN). The sample-to-detector distance was set to 1.6 meters and the incident neutron wavelength,  $\lambda$ , at 4-8 Å, resulting in a q-range of 0.02-0.8 Å<sup>-1</sup>, where q is the scattering vector and is determined as follows:

$$q = \frac{4\pi \sin\theta}{\lambda}, \quad (1)$$

where  $2\theta$  is the angle of scattered neutrons with respect to the incident beam. 1 mm path length quartz banjo cells (Hellma USA, Plainview, NY) used and neutrons were measured using a were collected and counted on a 2D <sup>3</sup>He detector. Scattering data were circularly av-

eraged to produce a 1D scattering intensity curve as a function of  $q$ . The data were corrected for empty cell and D<sub>2</sub>O background, sample transmission, and detector pixel sensitivity using the ORNL Mantid software.<sup>44</sup>

aLUVs with and without peptides were studied using SANS to determine lipid flip-flop rates. Flip-flop rates in the presence of pHLIP at different pH conditions were also studied. Lipid samples of 17 mg/mL concentration were measured at 37 °C for one hour to collect sufficient counting statistics high- $q$ .

**Modeling and Quantifying Lipid Flip-Flop Rates.** During SANS measurements, neutron scattered intensity  $I(q)$  was monitored as a function of  $q$ . At low- $q$ ,  $I(q)$  is dominated by the size and shape of the LUVs, while at high- $q$  the signal is primarily due to the average structure normal to the plane of the bilayer (e.g. bilayer thickness). In our case, the scattered intensity at high- $q$  is enhanced by the interleaflet contrast due to bilayer asymmetry, as shown in Fig. 1.

A normalized intensity decay scheme was used to quantify changes in scattered intensity as a function of time, as given by the normalized total intensity,  $\Delta I(t)/\Delta I(0)$ ,<sup>32</sup>

$$\frac{\Delta I(t)}{\Delta I(0)} = \frac{\sqrt{I(t)} - \sqrt{I(\infty)}}{\sqrt{I(0)} - \sqrt{I(\infty)}}, \quad (2)$$

where  $I(t)$  is the integrated area underneath the scattering curve at time  $t$  after the start of experimentation.  $I(0)$  and  $I(\infty)$  represent, respectively, the integrated area at  $t = 0$  of an aLUV sample and after bilayer asymmetry is lost. **The  $I(\infty)$  time-point is of the same lipid composition as our time-resolved samples, but the lipids are homogeneously mixed instead of asymmetrically distributed.** Because we are interested in observing changes to the bilayer as a result of lipid flip-flop, the total scattering intensity at each time point was determined by integrating the area under the scattered signal in the  $q$ -range 0.1 to 0.4 Å<sup>-1</sup>, where the difference in scattering intensity of asymmetric and symmetric LUVs is most pronounced. Plotting the normalized intensities as a function of time results in a decay curve that can be fitted using one parameter to determine the lipid flip-flop rate constant,  $k_f$ , i.e.

$$\frac{\Delta I(t)}{\Delta I(0)} = e^{(-2k_f t)}, \quad (3)$$

The flip-flop half time is then calculated as

$$t_{1/2} = \frac{\ln 2}{2k_f}. \quad (4)$$

## Determining Secondary Peptide Structure using Circular Dichroism.

Circular dichroism (CD) was used to determine the secondary structure of the different peptides after SANS and SAXS experimentation (see Fig. S3). CD spectra were acquired using a Jasco (Easton, MD) J-815 spectropolarimeter equipped with a Peltier system. Spectra were acquired at 37°C using a 2 mm cuvette at a scan rate of 100 nm/min, recording 20-40 acquisitions. The final lipid concentration was 1 mM. Raw data were converted into a mean residue ellipticity using

$$[\theta] = \frac{\theta}{10lc(N-1)}, \quad (5)$$

where  $\theta$  is the measured ellipticity,  $l$  is the path length of the cell in cm,  $c$  is the protein concentration in M, and  $N$  is the number of amino acids. Appropriate lipid blanks were subtracted in all cases.

## Results

### Lipid flip-flop can be monitored with SANS using asymmetric vesicles with interleaflet hydrogen/deuterium contrast

To monitor lipid flip-flop using time-resolved SANS, we first sought to determine if major scattering differences exist between aLUVs and symmetric LUVs. It is well-known that the

aLUV scattering form factor has minima with non-zero intensity, in contrast to that of symmetric LUVs.<sup>45</sup> Previous studies have used this feature to identify lipid asymmetry and build models to fit such data, extracting key bilayer parameters and leaflet compositions.<sup>29,30,46</sup>

Fig. 1b shows modeled  $I(q)$  curves based on LUVs with equal fractions of dH-POPC (deuterated headgroup) and dC-DMPC (perdeuterated acyl chains) at 37 °C. The model accounts for the scattering contributions from the individual bilayer leaflets.<sup>30</sup> Fig. 1b shows a substantial intensity increase in the  $q$ -range 0.15 - 0.3 Å<sup>-1</sup> for bilayers containing an asymmetric distribution of dH-POPC in the inner leaflet and dC-DMPC in the outer leaflet. To demonstrate this experimentally, we produced different model systems in order to mimic and maximize the dynamic range observed between the modeled asymmetric and symmetric curves. These systems possessed either isotopic asymmetry, i.e. the same lipid species but different isotopic labeling (not shown), or compositional asymmetry, where the individual leaflets possess chemically different lipid species.

Of the different samples studied, the aLUVs composed of dH-POPC<sup>inn</sup>/dC-DMPC<sup>out</sup> (Fig. 1a) possessed the greatest dynamic scattering range, as can be seen from the high- $q$  data (0.1 - 0.4 Å<sup>-1</sup>) shown in Fig. 1c. Compared to its relatively featureless scrambled counterpart, these aLUVs display appreciable “uplift” in scattering intensity in the vicinity of the first minima ( $\sim 0.18$  Å<sup>-1</sup>), which we attribute to the asymmetric distribution of lipids with different chemical makeups (Fig. 1b). This dynamic range was deemed suitable to monitor the bilayer transition from asymmetric to symmetric. Importantly, the modeled data bears a strong resemblance to the experimental data (Fig. 1b) and any minor differences can be attributed to potential deviations in lipid composition, bilayer thickness, polydispersity, and background scattering between the model and experimental.

**A transmembrane peptide pre-incorporated into asymmetric vesicles increases the rate of lipid flip-flop**

Control aLUVs and aLUVs with gA pre-incorporated were prepared separately, yet both scatter similarly as a function of  $q$  (Fig. 1c). This finding, coupled with the minimal loss

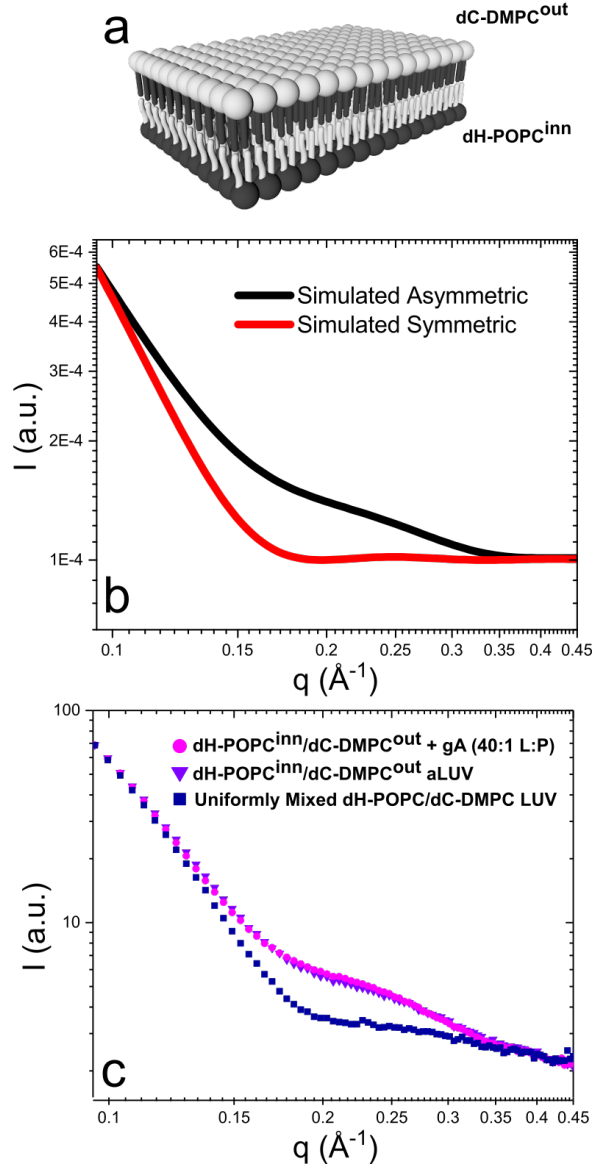


Figure 1: (a) Cartoon of an asymmetric bilayer. Dark shaded components indicates deuterated moieties. (b) Predicted neutron scattering curves of asymmetric ( $dH-POPC^{inn}/dC-DMPC^{out}$ ) and symmetric vesicles calculated using a six-slab bilayer model.<sup>30</sup> (c)  $I(q)$  scattering data from three different samples: (1) compositionally asymmetric LUVs with their inner leaflets composed mainly of  $dH-POPC$  and outer leaflet of  $dC-DMPC$  (pink circles); (2) aLUVs with a 1/40 P/L ratio of gA (purple triangles); and (3) uniformly mixed LUVs with same  $dH-POPC$  and  $dC-DMPC$  ratios (navy squares). Scattering curves are overlaid to highlight similarities and differences.

of gA seen in this type of asymmetric proteoliposome preparation,<sup>10</sup> lends confidence for this method of sample preparation for studies using SANS. It was also observed that gA in its transmembrane state does not contribute noticeably to the neutron scattering intensity,

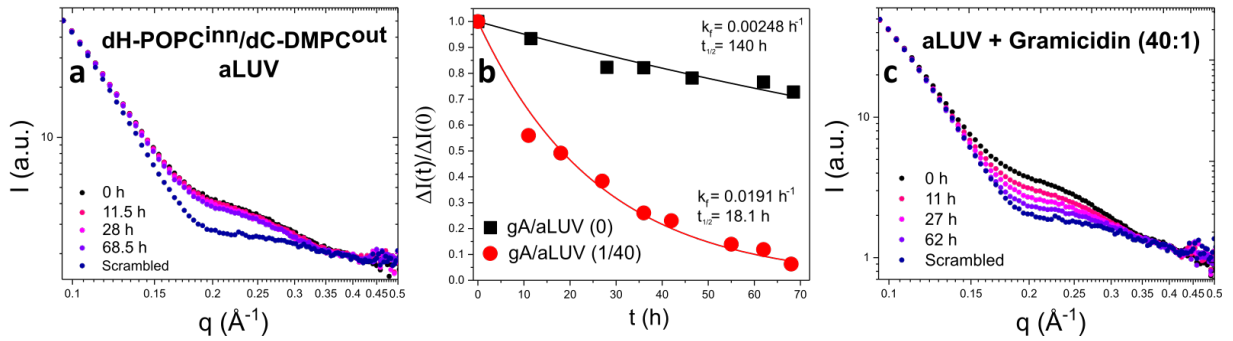


Figure 2: High- $q$  SANS data as a function of time showing an aLUV control (peptide-free, a). All measurements were conducted at 37 °C for one hour. For clarity purposes, not all measured curves are shown. (b) Normalized total intensity decay as a function of time in hours. Two plots are shown: aLUVs in the absence (black squares) and presence of gA (red circles) (P/L ratio of 1/40). Decays are the result of passive and peptide-enhanced lipid flip-flop, respectively. Continuous bold lines are best fits to the data used to determine the flip-flop rate constant ( $k_f$ ) and flip-flop half-time ( $t_{1/2}$ ). (c) Gramicidin-incorporated aLUVs at a P/L of 1/40.

meaning the measured ensemble average of the bilayer structure is unchanged. Although it is known that gA causes bilayer thinning or thickening depending on the conditions,<sup>47</sup> these deformations are likely to occur locally and, as a result, could not be detected by SANS in the present study or SAXS previously.<sup>10</sup>

Over the course of almost 3 days, the leaflet compositions of unperturbed fluid-phase aLUVs are practically unaltered as the aLUV scattering intensity data only show a slight decay (Fig. 2a). Because a complete minima decay was not collected, due to experimental time constraints often associated with SANS experimentation, an  $I(\infty)$  time-point (representing a homogeneously mixed LUV of the same overall lipid composition, as shown in Fig. 2) was used to normalize the integrated area of the intensity curves. Fits using equation 3 on the normalized integrated intensity from Fig. 2a revealed a flip-flop rate constant of  $2.48 \times 10^{-3} \text{ h}^{-1}$ , as shown in Fig. 2b. Converting the flip-flop rate constant to half-time using equation 4, the calculated half-time of 140 hours for peptide-free aLUVs is in good agreement with previous NMR results,<sup>10</sup> albeit slower than those found with LUVs doped with fluorescent or spin labelled lipids<sup>18,19,48</sup> and orders of magnitude slower than the rates

reported for supported bilayers.<sup>22-24</sup> When compared to the flip-flop half-times found by Nakano *et al.* in free-floating vesicles (DMPC  $t_{1/2} = \sim 8.5$  h, POPC  $t_{1/2} > 1000$  h both at 37 °C),<sup>32,33</sup> our aLUVs display a  $t_{1/2}$  much slower than pure DMPC, but slightly faster than flip-flop in POPC vesicles.

As shown in Fig. 2c, pre-incorporation of gA into aLUVs resulted in an accelerated decay of the scattered intensity, indicative of a continuous loss of membrane asymmetry. Fitting the normalized integrated total intensity showed that the presence of transmembrane gA reduced the flip-flop halftime from 140 h to 18.1 h – an almost 8-fold reduction in  $t_{1/2}$  and in good agreement with differential scanning calorimetry and NMR data.<sup>10</sup>

### **Externally added peptides result in rapid and complete loss of lipid asymmetry**

We also carried out experiments where aLUV controls were mixed either with Mel, Alm or pHLIP (at 3 different pH values) to determine the effects of membrane-surface events (such as binding and insertion) on bilayer asymmetry. Interestingly, the scattering curves did not decay in the same manner as observed with gA. In fact, the aLUV-peptide curves in Fig. 3a-e resemble those of the scrambled LUV control, i.e. the aLUVs lost their asymmetry within the first hour after preparation. The key differences between them are the method of peptide addition and peptide species: gA was incorporated during aLUV formation, Mel and Alm (Fig. 3a-b, respectively) introduced to aLUVs using d-methanol, and pHLIP powder to aLUVs in phosphate buffer with the addition of DCl to adjust the pH ((Fig. 3c-e). Regardless, the samples, where the peptide was added externally after the aLUVs were prepared, display the same effects on aLUV scattering. Specifically, bilayer asymmetry was affected over the same time period, regardless of differences in the peptide’s physical state or concentration, solvent type, pH, or mode of action.

As we altered pHLIP’s orientation from surface-bound to partially inserted and then to inserted (as indicated by CD, see Fig. S3), we observe the same bilayer scrambling effects of the PC lipids, which is depicted in Fig. 3c-e. It therefore appears that bilayer scrambling

results from an event that is not associated with pHLIP’s secondary structure or membrane partitioning. In pHLIP’s case, lipid flip-flop appears to be headgroup dependent as previous results have suggested that pHLIP does not promote flip-flop of PS lipids.<sup>9</sup> We rationalize this by the fact that PS and pHLIP are both negatively charged and thus repel each other.<sup>49</sup> Since only PS distribution was monitored in the previous study, the effect of pHLIP on PC flip-flop was not elucidated.

We also looked into any potential loss of asymmetry as a result of having methanol in solution. Using time-resolved SANS and symmetric protiated and deuterated DMPC vesicles, we previously showed that methanol at volumes as low as 0.5% increases the rate of DMPC vesicle mixing, and, in turn, DMPC flip-flop.<sup>50</sup> In those experiments, liposomal mixtures were incubated with methanol for one hour prior to mixing of the two isotopic DMPC populations. Aiming to learn whether enhanced lipid dynamics also occur in aLUVs, the maximum administered volume (3% v/v) of methanol, used to introduce Alm and Mel, was added to peptide-free aLUVs. Here, the introduction of methanol was followed by SANS measurement to capture any immediate lipid scrambling. The resulting SANS scattering pattern revealed no substantial decay in the first SANS minima (see Fig. S4), which indicates that methanol is not the primary driver of bilayer scrambling, pointing instead to a predominantly peptide-mediated mechanism of lipid flip-flop observed in this study. The present result is not necessarily a contradiction to our past work. One hour (the time aLUV samples were measured on SANS here) of data collection only produces 10-20% of the total intensity decay curve in pure symmetric DMPC vesicles.<sup>50</sup> In other words, in both symmetric and asymmetric instances, d-methanol did not initiate an immediate and complete scrambling of lipid bilayers. **To note, samples containing gA and pHLIP were methanol-free.**

To further verify that peptides were the primary cause of lipid scrambling, we monitored for the possibility of vesicle fusion, which can potentially increase the rate of lipid bilayer scrambling. Besides pHLIP,<sup>41</sup> the other peptides studied are known to promote vesicle fusion,<sup>51</sup> especially at concentrations of  $P/L \geq 1/50$ .<sup>52</sup> However, DLS measurements taken

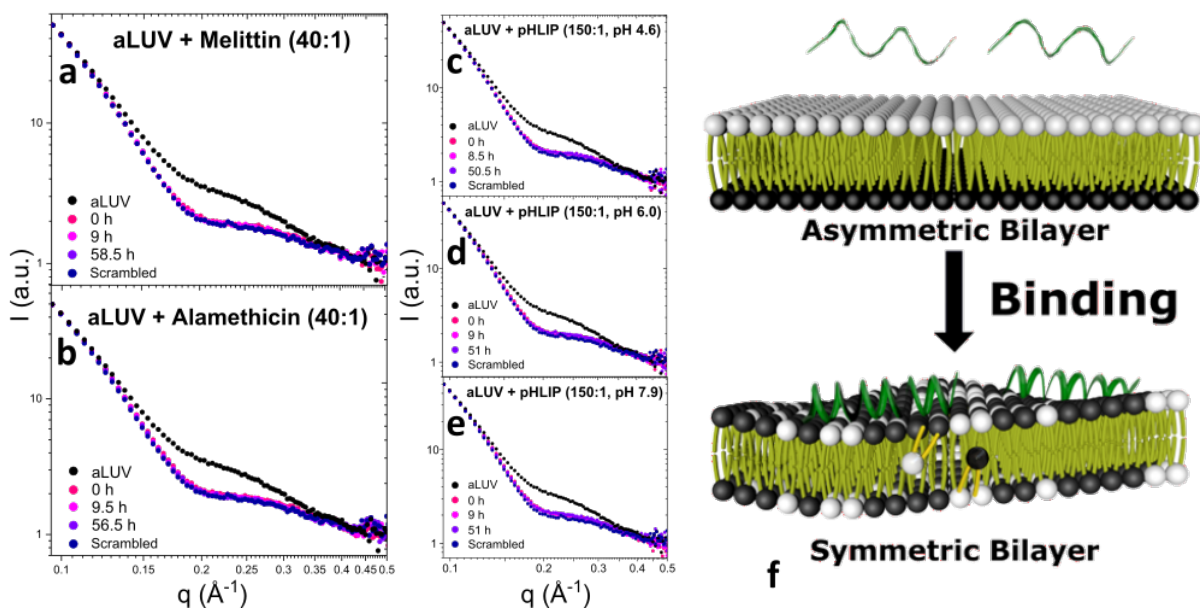


Figure 3: (a-e) High- $q$  SANS data as a function of time showing aLUV scattering curves after the external addition of melittin (a), alamethicin (b), and pHLIP (c-e). The individual L/P ratios are displayed in each graph. All measurements were conducted at 37 °C. For clarity purposes, not all measured curves are shown. (f) Cartoon of proposed mechanism of peptide-induced lipid flip-flop. Shown in the top panel of (f) are the peptide monomers in a random coil conformation and an asymmetric bilayer composed of chemically distinct leaflets. Peptide binding, shown in the bottom, initiates a conformational change from a random coil to  $\alpha$ -helical. This adsorption, and likely subsequent insertion events leads to bilayer reorganization and loss of lipid asymmetry.

prior to peptide addition and after incubation dismiss this possibility, as the average particle diameter was unaffected (data not shown). This result also rules out the “carpet” mechanism where vesicles disintegrate into polydisperse peptidolipid structures.<sup>53</sup> We can thus confidently conclude that the observed changes in scattering are due to lipid flip-flop and not the result of large-scale structural reorganization.

## Discussion

As mentioned, the externally added peptides interact with the membrane through very different mechanisms. However, regardless of their mode of action, amino acid sequence, length, and conformation, they all disrupt membrane asymmetry, hinting at a general mode

of action. Even though pHLIP is not an AMP, it is possible that pHLIP and AMPs share certain features that allow them to disrupt membrane asymmetry despite differences in how they interact with membranes. Our findings point to this scenario – one which implies that perhaps all natural and *de novo* peptides and proteins may be capable of causing substantial lipid flip-flop.

It has been suggested that any membrane-interacting molecules, at sufficient quantities, are able to influence membrane properties<sup>54</sup> by compromising the mechanical integrity of the bilayer. Therefore, at high peptide-to-lipid ( $P/L \geq 1/40$ ) concentrations, changes to the membrane may be due to an overwhelming number of peptides interacting simultaneously with the membrane and not necessarily a specific AMP mode of action. However, with respect to the current study, the non-pore forming pHLIP at a P/L ratio of 1/150 refutes this possibility. At this non-membrane permeabilizing concentration,<sup>55</sup> the peptide was seen to eliminate membrane asymmetry, while the presence of gA in the membrane at higher concentrations ( $P/L = 1/40$ ) did not rapidly scramble the bilayers. Instead, we observed a gradual loss of asymmetry. Our data therefore suggest that the enhanced lipid flip-flop observed for pHLIP, Alm, and Mel is related to their activity at the membrane surface (see Fig. 3f).

For lytic AMPs, an initial mode of action involves interaction with cellular membranes. Most AMPs begin in the aqueous extracellular matrix as randomly coiled monomers and undergo a conformational change upon contact with the membrane, forming a variety of secondary structures that allow for peptide penetration and eventual membrane permeation. However, few studies have looked into the potential of peptide binding to the membrane as a disrupter of lipid asymmetry. Fattal *et al.* suggested that if a “perturbation mode” of action (also known as *interfacial activity*, where peptides in a non-oligomeric, surface-bound state disturb the physicochemical properties of adjacent lipids<sup>54</sup>) indeed existed, lipid flip-flop would occur upon peptide binding to the bilayer<sup>12</sup> – a notion in agreement with the data presented in the current study. Decoupling the binding and transmembrane steps

showed that the peptides that underwent a binding step initiated rapid and complete lipid asymmetry loss, in contrast to the gA case.

At similar P/L concentrations, gA did not cause 7-nitrobenz-2-oxa-1,3-diazol-4-yl (NBD) conjugated PC lipids to experience “appreciable” lipid flip-flop<sup>12</sup>(> 96 h), suggesting gA is better capable of enhancing the translocation of biologically relevant lipids than those modified covalently. This difference can be attributed either to an unfavorable steric interaction between the NBD fluorophore and the peptide, or that the bulkiness of the fluorophore impede movement through the peptide-induced defect. In Fig. 2b, gA (18.1 h) and gA-free (140 h) half-times show an almost 8-fold decrease when gA is pre-incorporated into aLUVs. This result is, for the most part, in good agreement with that of Anglin and coworkers (2-10 fold increase in gel-phase di18:0 PC bilayers). The similarity in time-scales (hours) yet difference in lipid phase-state (fluid vs. gel) is intriguing as the rate of lipid flip-flop has been shown to be phase-dependent<sup>18,25</sup> – with flip-flop in gel-phase membranes being much slower. Bilayer geometry, incomplete surface coverage in planar bilayers, and possible substrate-lipid interactions in supported bilayers are possible explanations for these difference in time-scales.<sup>14,25,36</sup> Nevertheless, gA activity appears to be independent of lipid phase state.

In its surface-adsorbed state, pHLIP can perturb lipid membranes to a greater extent than when inserted.<sup>55</sup> This may also be true for Alm and Mel, which can adopt a surface-bound state.<sup>56</sup> In their monomeric forms, Alm and Mel are embedded just below the lipid headgroups, lying parallel to the membrane plane (not inserted).<sup>57</sup> In this surface-bound state, they induce membrane thinning<sup>57</sup> that can compromise membrane integrity by creating local defects that can accelerate lipid flip-flop – a notion that is in agreement with previous reported findings.<sup>25,58</sup>

A surface-adsorbed peptide that lies below the headgroups would change the effective area of that (outer) leaflet, which would lead to global stresses across the membrane. This area imbalance may then result in disruption of the sustained partitioning of the hydrophobic and hydrophilic regions present in the bilayer, allowing for the transbilayer movement of

solutes, peptides, and lipids.<sup>54</sup> This type of stress (normal to the bilayer plane) is different from that produced by gA, possibly leading to the different outcomes observed here. As previously described,<sup>10</sup> gA-induced stress (directed radially outwards from the transmembrane peptide) comes from the high gA concentration ( $P/L = 1/40$ ) at which, because of the local deformations around gA, the bilayer is unable to relax to its unperturbed state, since the gA dimers are too close to one another. These local deformations enhance the formation of defects, which reduces the free energy barrier to lipid flip-flop by destabilizing adjacent bilayer structure and/or lipid packing near the peptide.<sup>10</sup> We postulate that the interfacial activity of a peptide on the membrane surface induces a far greater stress upon the bilayer than when in its transmembrane state. This postulation is corroborated by a finding in which the number of lipids affected by adsorbed pHLIP is a factor of  $\sim 5-10$  greater than transmembrane pHLIP.<sup>59</sup> We thus believe there exists a direct correlation between the amount of stress induced by the peptide (which seems dependent on its orientation) and its ability to propagate lipid flip-flop events.

At a critical P/L concentration, AMPs will transition from laying on the membrane surface to inserting themselves into the membrane, spanning both bilayer leaflets.<sup>56</sup> In the present study, Alm and Mel are seen to primarily adopt an  $\alpha$ -helical structure and thus inserted orientation (see Fig. S3). This is significant, as what was suggested previously,<sup>16</sup> the act of peptide insertion can help transfer lipids across bilayer leaflets as lipids can be co-transported with the plunging peptide. Along with the potential for dynamic conversion between inserted and non-inserted states, the co-transport process should be very effective at disrupting lipid organization.

This insertion step, as well as membrane binding, is missing in the case of gA as it was already pre-incorporated into the bilayer. We speculate that adding gA externally would yield similar results on the basis that the other three peptides examined differ drastically in amino acid composition and sequence length. Furthermore, as seen with pHLIP, a specific secondary structure and pore-formation are not pre-requisites to causing complete lipid

scrambling; thus, the delayed formation of helical gA channels (due to the accumulation of gA on the outer leaflet, instead of being present on both leaflets) would not affect the bilayer scrambling process as gA inserts itself into the bilayer.

An interesting point to note, with regards to the flip-flop halftime measured here for POPC and DMPC aLUVs, the observed value of  $\sim 140$  h is magnitudes slower than in pure DMPC LUVs<sup>32</sup> and faster than the imperceptible POPC flip-flop<sup>33</sup>. Taking into consideration interleaflet coupling<sup>8</sup>, we suggest that the POPC-enriched leaflet may suppress lipids in the DMPC-enriched leaflet from flipping inward, giving rise to the observed half-time. Lipid flip-flop is known to be affected by bilayer thickness, among other properties<sup>8,18</sup>. In this case, either the thicker POPC inner leaflet is inhibiting DMPC from flipping inwards or, because POPC is not undergoing lipid flip-flop, there is an equal exchange of DMPC between the leaflets to compensate for any leaflet area imbalance, resulting in a lack of net change in leaflet composition. The equal exchange of DMPC between leaflets, is possible because some outer leaflet lipids will leak into the inner leaflet during aLUV formation ( $\sim 5-10\%$ ), allowing for the bidirectional diffusion of DMPC. Ultimately, the introduction of lipid asymmetry is seen to influence both POPC and DMPC translocation rates.

Though the current study does not provide unequivocal support for a peptide-based mechanism of lipid flip-flop, it does provide insights regarding membrane-peptide interactions affecting bilayer asymmetry and their possible importance in biological membranes. AMP action does not always lead to complete membrane destruction, which has clearly been demonstrated by the present SANS and DLS data. In search of another plausible mechanism, we delved into the action of AMPs onto lipids, specifically their dynamics and overall organization within the bilayer. Complete lipid scrambling of asymmetrically organized lipid bilayers was found. For lipid scrambling to be of biological relevance in the action of AMPs, a fast, or even immediate, effect is needed and desirable – one which precedes the permeabilization of the membrane. This study shows that such a case is possible. Our findings also reveal the importance of evaluating vesicle asymmetry in studies involving peptides and

proteins as peptide reconstitution was shown to destabilize the organizational integrity of aLUVs.

## Conclusions

Although there are a number of different techniques that can measure lipid flip-flop, there are few that can do so in a probe-free and non-headgroup specific manner. Here, we demonstrated how SANS could be used to reliably monitor lipid flip-flop in aLUVs made of dH-POPC<sup>inn</sup>/dC-DMPC<sup>out</sup>. In these vesicles, lipid flip-flop half-times approaching 6 days were observed, in good agreement with some previous results and in contrast with those obtained from supported bilayers. The pre-incorporation of gA into aLUVs increased lipid flip-flop rates by a factor of almost 8, compared to peptide-free aLUVs. The addition of Alm, Mel and pHLIP (at three different pH conditions) also eliminated membrane asymmetry. Importantly, it was shown that peptides adsorbed to membrane surfaces may have a much greater effect on lipid flip-flop than when inserted. This result highlighted a possible general mechanism of AMP action, which may be important to initiating cell death.

## Acknowledgement

Part of this research was conducted at ORNL's Spallation Neutron Source, sponsored by the Scientific User Facilities Division, Office of Basic Energy Sciences, U.S. Department of Energy. SAXS, DLS, and NMR measurements were supported by DOE scientific user facilities. This work was funded, in part, by the University of Windsor startup funds to DM. MD and MHLN are both supported by Ontario Graduate Scholarships (OGS). DM acknowledges the support of the Natural Sciences and Engineering Research Council of Canada (NSERC), [funding reference number 2018-04841]. This work was partially supported by NIH grant R01GM120642 (FNB) and NSF grant MCB-1817929 (FAH). JK is supported through the Scientific User Facilities Division of the Department of Energy (DOE) Office of Science, spon-

sored by the Basic Energy Science (BES) Program, DOE Office of Science, under Contract No. DEAC05-00OR22725.

## Supporting Information Available

Detailed experimental results, and theory can be found in Supporting Information.

## References

- (1) Manno, S.; Takakuwa, Y.; Mohandas, N. Identification of a functional role for lipid asymmetry in biological membranes: Phosphatidylserine-skeletal protein interactions modulate membrane stability. *Proceedings of the National Academy of Sciences* **2002**, *99*, 1943–1948.
- (2) Lhermusier, T.; Chap, H.; Payrastre, B. Platelet membrane phospholipid asymmetry: from the characterization of a scramblase activity to the identification of an essential protein mutated in Scott syndrome. *Journal of Thrombosis and Haemostasis* **2011**, *9*, 1883–1891.
- (3) Seigneuret, M.; Devaux, P. F. ATP-dependent asymmetric distribution of spin-labeled phospholipids in the erythrocyte membrane: relation to shape changes. *Proceedings of the National Academy of Sciences of the United States of America* **1984**, *81*, 3751–5.
- (4) Martin, S. J. Early redistribution of plasma membrane phosphatidylserine is a general feature of apoptosis regardless of the initiating stimulus: inhibition by overexpression of Bcl-2 and Abl. *Journal of Experimental Medicine* **1995**, *182*, 1545–1556.
- (5) Zwaal, R. F. A. Membrane and lipid involvement in blood coagulation. *BBA - Reviews on Biomembranes* **1978**, *515*, 163–205.

- (6) Kamiya, K.; Kawano, R.; Osaki, T.; Akiyoshi, K.; Takeuchi, S. Cell-sized asymmetric lipid vesicles facilitate the investigation of asymmetric membranes. *Nature chemistry* **2016**, *8*, 881.
- (7) Yanagisawa, M.; Iwamoto, M.; Kato, A.; Yoshikawa, K.; Oiki, S. Oriented reconstitution of a membrane protein in a giant unilamellar vesicle: experimental verification with the potassium channel KcsA. *Journal of the American Chemical Society* **2011**, *133*, 11774–11779.
- (8) Marquardt, D.; Geier, B.; Pabst, G. Asymmetric lipid membranes: towards more realistic model systems. *Membranes* **2015**, *5*, 180–196.
- (9) Scott, H. L.; Heberle, F. A.; Katsaras, J.; Barrera, F. N. Phosphatidylserine Asymmetry Promotes the Membrane Insertion of a Transmembrane Helix. *Biophysical Journal* **2019**, *116*, 1495–1506.
- (10) Doktorova, M.; Heberle, F. A.; Marquardt, D.; Rusinova, R.; Sanford, R. L.; Peyear, T. A.; Katsaras, J.; Feigenson, G. W.; Weinstein, H.; Andersen, O. S. Gramicidin Increases Lipid Flip-Flop in Symmetric and Asymmetric Lipid Vesicles. *Biophys. J.* **2019**, *116*, 860–873.
- (11) Béven, L.; Wroblewski, H. Effect of natural amphipathic peptides on viability, membrane potential, cell shape and motility of mollicutes. *Research in microbiology* **1997**, *148*, 163–175.
- (12) Fattal, E.; Parente, R. A.; Szoka, F. C.; Nir, S. Pore-Forming Peptides Induce Rapid Phospholipid Flip-Flop in Membranes. *Biochemistry* **1994**, *33*, 6721–6731.
- (13) Taylor, G.; Nguyen, M. A.; Koner, S.; Freeman, E.; Collier, C. P.; Sarles, S. A. Electrophysiological interrogation of asymmetric droplet interface bilayers reveals surface-bound alamethicin induces lipid flip-flop. *Biochimica et Biophysica Acta - Biomembranes* **2019**, *1861*, 335–343.

- (14) Anglin, T. C.; Liu, J.; Conboy, J. C. Facile lipid flip-flop in a phospholipid bilayer induced by gramicidin A measured by sum-frequency vibrational spectroscopy. *Biophys. J.* **2007**, *92*, L01–3.
- (15) Sapay, N.; Bennett, W. F.; Tieleman, D. P. Molecular simulations of lipid flip-flop in the presence of model transmembrane helices. *Biochemistry* **2010**, *49*, 7665–7673.
- (16) Matsuzaki, K.; Murase, O.; Fujii, N.; Miyajima, K. An antimicrobial peptide, magainin 2, induced rapid flip-flop of phospholipids coupled with pore formation and peptide translocation. *Biochemistry* **1996**, *35*, 11361–11368.
- (17) Hwang, B.; Hwang, J. S.; Lee, J.; Kim, J. K.; Kim, S. R.; Kim, Y.; Lee, D. G. Induction of yeast apoptosis by an antimicrobial peptide, Papiliocin. *Biochemical and Biophysical Research Communications* **2011**, *408*, 89–93.
- (18) John, K.; Schreiber, S.; Kubelt, J.; Herrmann, A.; Müller, P. Transbilayer Movement of Phospholipids at the Main Phase Transition of Lipid Membranes: Implications for Rapid Flip-Flop in Biological Membranes. *Biophys. J.* **2002**, *83*, 3315–3323.
- (19) Kornberg, R. D.; McConnell, H. M. Inside-outside transitions of phospholipids in vesicle membranes. *Biochemistry* **1971**, *10*, 1111–1120.
- (20) Kol, M. A.; van Laak, A. N. C.; Rijkers, D. T. S.; Killian, J. A.; de Kroon, A. I. P. M.; de Kruijff, B. Phospholipid Flop Induced by Transmembrane Peptides in Model Membranes Is Modulated by Lipid Composition. *Biochemistry* **2003**, *42*, 231–237.
- (21) Devaux, P. F.; Fellmann, P.; Hervé, P. Investigation on lipid asymmetry using lipid probes: Comparison between spin-labeled lipids and fluorescent lipids. *Chemistry and Physics of Lipids* **2002**, *116*, 115–134.
- (22) Liu, J.; Conboy, J. C. 1,2-diacyl-phosphatidylcholine flip-flop measured directly by sum-frequency vibrational spectroscopy. *Biophys. J.* **2005**, *89*, 2522–2532.

- (23) Anglin, T. C.; Cooper, M. P.; Li, H.; Chandler, K.; Conboy, J. C. Free energy and entropy of activation for phospholipid flip-flop in planar supported lipid bilayers. *J. Phys. Chem. B.* **2010**, *114*, 1903–1914.
- (24) Gerelli, Y.; Porcar, L.; Lombardi, L.; Fragneto, G. Lipid Exchange and Flip-Flop in Solid Supported Bilayers. *Langmuir* **2013**, *29*, 12762–12769.
- (25) Marquardt, D.; Heberle, F. A.; Miti, T.; Eicher, B.; London, E.; Katsaras, J.; Pabst, G. <sup>1</sup>H NMR Shows Slow Phospholipid Flip-Flop in Gel and Fluid Bilayers. *Langmuir* **2017**, *33*, 3731–3741.
- (26) Nickels, J. D.; Chatterjee, S.; Stanley, C. B.; Qian, S.; Cheng, X.; Myles, D. A. A.; Standaert, R. F.; Elkins, J. G.; Katsaras, J. The in vivo structure of biological membranes and evidence for lipid domains. *PLoS Biology* **2017**, *15*, e2002214.
- (27) Murugova, T. N.; Solodovnikova, I. M.; Yurkov, V. I.; Gordeliy, V. I.; Kuklin, A. I.; Ivankov, O. I.; Kovalev, Y. S.; Popov, V. I.; Teplova, V. V.; Yaguzhinsky, L. S. Potentials of Small-angle Neutron Scattering for Studies of the Structure of Live Mitochondria. *Neutron News* **2011**, *22*, 11–14.
- (28) Norbert Kučerka,; Mu-Ping Nieh,; John Katsaras, Fluid phase lipid areas and bilayer thicknesses of commonly used phosphatidylcholines as a function of temperature. *Biochim. Biophys. Acta.* **2011**, *1808*, 2761–2771.
- (29) Heberle, F. A.; Marquardt, D.; Doktorova, M.; Geier, B.; Standaert, R. F.; Heftberger, P.; Kollmitzer, B.; Nickels, J. D.; Dick, R. A.; Feigenson, G. W.; Katsaras, J.; London, E.; Pabst, G. Sub-nanometer Structure of an Asymmetric Model Membrane: Interleaflet Coupling Influences Domain Properties. *Langmuir* **2016**, *32*, 5195–5200.
- (30) Eicher, B.; Heberle, F. A.; Marquardt, D.; Rechberger, G. N.; Katsaras, J.; Pabst, G. Joint small-angle X-ray and neutron scattering data analysis of asymmetric lipid vesicles. *Journal of Applied Crystallography* **2017**, *50*.

- (31) Nielsen, J. E.; Bjørnstad, V. A.; Lund, R. Resolving the Structural Interactions between Antimicrobial Peptides and Lipid Membranes using Small-angle Scattering Methods: the case of Indolicidin. *Soft Matter* **2018**,
- (32) Nakano, M.; Fukuda, M.; Kudo, T.; Endo, H.; Handa, T. Determination of interbilayer and transbilayer lipid transfers by time-resolved small-angle neutron scattering. *Physical review letters* **2007**, *98*, 238101.
- (33) Nakano, M.; Fukuda, M.; Kudo, T.; Matsuzaki, N.; Azuma, T.; Sekine, K.; Endo, H.; Handa, T. Flip-flop of phospholipids in vesicles: kinetic analysis with time-resolved small-angle neutron scattering. *J. Phys. Chem. B* **2009**, *113*, 6745–6748.
- (34) Garg, S.; Porcar, L.; Woodka, A. C.; Butler, P. D.; Perez-Salas, U. Noninvasive Neutron Scattering Measurements Reveal Slower Cholesterol Transport in Model Lipid Membranes. *Biophysical Journal* **2011**, *101*, 370–377.
- (35) Sugiura, T.; Takahashi, C.; Chuma, Y.; Fukuda, M.; Yamada, M.; Yoshida, U.; Nakao, H.; Ikeda, K.; Khan, D.; Nile, A. H.; Bankaitis, V. A.; Nakano, M. Biophysical Parameters of the Sec14 Phospholipid Exchange Cycle. *Biophysical Journal* **2019**, *116*, 92–103.
- (36) Wah, B.; Breidigan, J. M.; Adams, J.; Horbal, P.; Garg, S.; Porcar, L.; Perez-Salas, U. Reconciling Differences between Lipid Transfer in Free-Standing and Solid Supported Membranes: A Time-Resolved Small-Angle Neutron Scattering Study. *Langmuir* **2017**, *33*, 3384–3394.
- (37) Doktorova, M.; Heberle, F. A.; Eicher, B.; Standaert, R. F.; Katsaras, J.; London, E.; Pabst, G.; Marquardt, D. Preparation of asymmetric phospholipid vesicles for use as cell membrane models. *Nature Protocols* **2018**, *13*, 2086–2101.
- (38) Peyret, A.; Zhao, H.; Lecommandoux, S. Preparation and Properties of Asymmetric

- Synthetic Membranes Based on Lipid and Polymer Self-Assembly. *Langmuir* **2018**, *34*, 3376–3385.
- (39) Bechinger, B. Structure and functions of channel-forming peptides: Magainins, cecropins, melittin and alamethicin. 1997.
- (40) Scott, H. L.; Westerfield, J. M.; Barrera, F. N. Determination of the Membrane Translocation pK of the pH-Low Insertion Peptide. *Biophysical Journal* **2017**, *113*, 869–879.
- (41) Reshetnyak, Y. K.; Segala, M.; Andreev, O. A.; Engelman, D. M. A monomeric membrane peptide that lives in three worlds: In solution, attached to, and inserted across lipid bilayers. *Biophysical Journal* **2007**, *93*, 2363–2372.
- (42) Musial-Siwiek, M.; Karabadzha, A.; Andreev, O. A.; Reshetnyak, Y. K.; Engelman, D. M. Tuning the insertion properties of pHLIP. *Biochimica et Biophysica Acta - Biomembranes* **2010**, *1798*, 1041–1046.
- (43) Eicher, B.; Marquardt, D.; Heberle, F. A.; Letofsky-Papst, I.; Rechberger, G. N.; Appavou, M. S.; Katsaras, J.; Pabst, G. Intrinsic Curvature-Mediated Transbilayer Coupling in Asymmetric Lipid Vesicles. *Biophysical Journal* **2018**, *114*, 146–157.
- (44) Arnold, O.; Bilheux, J. C.; Borreguero, J. M.; Buts, A.; Campbell, S. I.; Chapon, L.; Doucet, M.; Draper, N.; Ferraz Leal, R.; Gigg, M. A.; Lynch, V. E.; Markvardsen, A.; Mikkelsen, D. J.; Mikkelsen, R. L.; Miller, R.; Palmen, K.; Parker, P.; Passos, G.; Perring, T. G.; Peterson, P. F.; Ren, S.; Reuter, M. A.; Savici, A. T.; Taylor, J. W.; Taylor, R. J.; Tolchenov, R.; Zhou, W.; Zikovsky, J. Mantid - Data analysis and visualization package for neutron scattering and  $\mu$  SR experiments. *Nuclear Instruments and Methods in Physics Research, Section A: Accelerators, Spectrometers, Detectors and Associated Equipment* **2014**, *764*, 156–166.
- (45) Kučerka, N.; Nieh, M.-P.; Katsaras, J. *Advances in planar lipid bilayers and liposomes*; Elsevier, 2010; Vol. 12; pp 201–235.

- (46) Qian, S.; Heller, W. T. Peptide-induced asymmetric distribution of charged lipids in a vesicle bilayer revealed by small-angle neutron scattering. *The Journal of Physical Chemistry B* **2011**, *115*, 9831–9837.
- (47) Harroun, T. A.; Heller, W. T.; Weiss, T. M.; Yang, L.; Huang, H. W. Experimental evidence for hydrophobic matching and membrane-mediated interactions in lipid bilayers containing gramicidin. *Biophysical Journal* **1999**, *76*, 937–945.
- (48) Anzai, K.; Yoshioka, Y.; Kirino, Y. Novel radioactive phospholipid probes as a tool for measurement of phospholipid translocation across biomembranes. *BBA - Biomembranes* **1993**, *1151*, 69–75.
- (49) Scott, H. L.; Nguyen, V. P.; Alves, D. S.; Davis, F. L.; Booth, K. R.; Bryner, J.; Barrera, F. N. The negative charge of the membrane has opposite effects on the membrane entry and exit of ph-low insertion peptide. *Biochemistry* **2015**, *54*, 1709–1712.
- (50) Nguyen, M.; DiPasquale, M.; Rickeard, B.; Stanley, C.; Kelley, E.; Marquardt, D. Methanol Accelerates DMPC Flip-Flop and Transfer: A SANS Study on Lipid Dynamics. *Biophysical Journal* **2019**, *116*, 755–759.
- (51) Gilbert, R. J. C. Proteinlipid interactions and non-lamellar lipidic structures in membrane pore formation and membrane fusion. *Biochimica et Biophysica Acta - Biomembranes* **2016**, *1858*, 487–499.
- (52) Rausch, J. M.; Marks, J. R.; Rathinakumar, R.; Wimley, W. C. B-Sheet pore-forming peptides selected from a rational combinatorial library: Mechanism of pore formation in lipid vesicles and activity in biological membranes. *Biochemistry* **2007**, *46*, 12124–12139.
- (53) Shai, Y. Mode of action of membrane active antimicrobial peptides. *Biopolymers - Peptide Science Section* **2002**, *66*, 236–248.

- (54) Wimley, W. C. Describing the mechanism of antimicrobial peptide action with the interfacial activity model. *ACS chemical biology* **2010**, *5*, 905–917.
- (55) Zoonens, M.; Reshetnyak, Y. K.; Engelman, D. M. Bilayer interactions of pHLIP, a peptide that can deliver drugs and target tumors. *Biophysical Journal* **2008**, *95*, 225–235.
- (56) Huang, H. W. Molecular mechanism of antimicrobial peptides: The origin of cooperativity. *Biochimica et Biophysica Acta - Biomembranes* **2006**, *1758*, 1292–1302.
- (57) Chen, F. Y.; Lee, M. T.; Huang, H. W. Evidence for membrane thinning effect as the mechanism for peptide-induced pore formation. *Biophysical Journal* **2003**, *84*, 3751–3758.
- (58) De Kruijff, B.; Van Zoelen, E. J. J. Effect of the phase transition on the transbilayer movement of dimyristoyl phosphatidylcholine in unilamellar vesicles. *BBA - Biomembranes* **1978**, *511*, 105–115.
- (59) Reshetnyak, Y. K.; Andreev, O. A.; Segala, M.; Markin, V. S.; Engelman, D. M. Energetics of peptide (pHLIP) binding to and folding across a lipid bilayer membrane. *Proceedings of the National Academy of Sciences* **2008**, *105*, 15340–15345.

# Graphical TOC Entry

